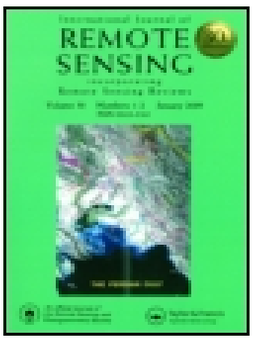

International Journal of Remote Sensing

ISSN: 0143-1161 (Print) 1366-5901 (Online) Journal homepage: https://www.tandfonline.com/loi/tres20

Characteristics of maximum-value composite images from temporal AVHRR data

BRENT N. HOLBEN

To cite this article: BRENT N. HOLBEN (1986) Characteristics of maximum-value composite images from temporal AVHRR data, International Journal of Remote Sensing, 7:11, 1417-1434, DOI: 10.1080/01431168608948945

To link to this article: https://doi.org/10.1080/01431168608948945

INT. J. REMOTE SENSING, 1986, VOL. 7, NO. 11, 1417–1434

Characteristics of maximum-value composite images from temporal AVHRR data

BRENT N. HOLBEN

Laboratory for Terrestrial Physics/Code 623, NASA/Goddard Space Flight Center, Greenbelt, Maryland 20771, U.S.A.

Abstract. Red and near-infrared satellite data from the Advanced Very High Resolution Radiometer sensor have been processed over several days and combined to produce spatially continuous cloud-free imagery over large areas with sufficient temporal resolution to study green-vegetation dynamics. The technique minimizes cloud contamination, reduces directional reflectance and off-nadir viewing effects, minimizes sun-angle and shadow effects, and minimizes aerosol and water-vapour effects. The improvement is highly dependent on the state of the atmosphere, surface-cover type, and the viewing and illumination geometry of the sun, target and sensor. An example from southern Africa showed an increase of 40 per cent from individual image values to the final composite image. Limitations associated with the technique are discussed, and recommendations are given to improve this approach.

1. Introduction

Visible and near-infrared remote sensing for Earth surface observation has historically been restricted to the analysis of a few scenes over selected areas owing to the presence of clouds, poor atmospheric conditions, infrequent satellite coverage, and high costs of data acquisition and processing. These factors combine to provide a temporally intermittent view of the Earth's surface and the dynamic changes that occur in vegetation communities over time. This paper evaluates the technical aspects of a processing methodology that uses Advanced Very High Resolution Radiometer (AVHRR) visible- and near-infrared-band satellite data to study dynamic processes of terrestrial vegetation while minimizing several problems associated with short-wave Earth-observing satellites. The National Oceanic and Atmospheric Administration's (NOAA) satellite series carrying the AVHRR has the spatial coverage and spectral resolution needed for monitoring green-vegetation dynamics globally on a daily basis (Gray and McCrary 1981, Townshend and Tucker 1981, Schneider and McGinnis 1982, Gatlin *et al.* 1981). A description of the NOAA AVHRR sensor characteristics is given by Justice *et al.* (1985). Daily global coverage is generated by the $\pm 56°$ across-track viewing and $\sim 1{\cdot}1$ km local-area coverage (LAC) and approximately 4 km global-area coverage (GAC) spatial resolutions. Global daily coverage is available only through the GAC data that are generated on board the satellite by partial resampling of the LAC data (Kidwell 1984, Townshend and Justice 1986). Although the AVHRR spectral channels were designed for cloud, atmospheric and sea-surface temperature analysis, the visible (VIS) and near-infrared (NIR) channels are also suitable for vegetation studies (Schneider and McGinnis 1982). In this context the data were first used globally in a ratio-composite framework to monitor green vegetation over time and to reduce the influence of cloud cover (Tarpley *et al.* 1984). The global vegetation index (GVI) is a standard NOAA product derived from seven continuous days of global GAC data resampled to about 20 km resolution and reprojected into a polar stereographic format. The composite procedure is based on the normalized

difference vegetation index (NDVI), which is a ratio of the NIR and visible radiances (NIR − VIS)/(NIR + VIS) (Deering *et al.* 1975). This ratio yields a measure of photosynthetic capacity such that the higher the value of the ratio, the more photosynthetically active the cover type (Sellers 1985). The maximum-value composite procedure (MVC), as it will be referred to here, requires that a series of multitemporal georeferenced satellite data be processed into NDVI images. On a pixel-by-pixel basis, each NDVI value is examined, and only the highest value is retained for each pixel location. A final MVC image is produced after all pixels have been evaluated.

The NOAA seven-day composite global vegetation index (GVI) has gone through several variations of this approach since its inception in April 1982 (NOAA 1983). Further development of the MVC procedure has been implemented by increasing the number of acquisitions to process a single composite image, i.e. up to 30 consecutive scenes (Tucker *et al.* 1984b, Justice *et al.* 1985), and by including a thermal cloud mask (Tucker *et al.* 1982, Gatlin *et al.* 1984). The thermal cloud mask eliminates NDVI data that have a temperature below a previously defined threshold. For most of GIMMS African work, the threshold was set at a 285 K brightness temperature in AVHRR channel 5 (10·5–11·5 μm). Because the African landmass is in the tropical latitudes, it was assumed that surface brightness temperatures would be above the threshold values even at high elevations during the afternoon AVHRR passes. Since cloud pixels typically have brightness temperatures less than the land surface, the threshold value of corresponding NDVI pixels is set at zero. A similar approach can be made using the 0·62–0·72 μm visible channel: assuming that clouds have a higher reflectance than the Earth's surface, a threshold value may be determined such that NDVI values above the visible threshold will be set at zero.

The combined approach of the MVC and the thermal cloud mask has been used with several studies involving NOAA-7 AVHRR data. Tucker *et al.* (1985a) have completed a monthly NDVI composite data set of Africa in which those data have been related to green biomass productivity. Other studies at smaller scales have related MVC and thermally masked AVHRR data sets to green vegetation dynamics and primary production (Tucker *et al.* 1983, 1984a, b, Goward *et al.* 1985, Justice *et al.* 1986). Furthermore, MVC and thermally masked data sets have been used for a vegetation classification of Africa (Tucker *et al.* 1985a), as well as to show the phenology of cultivated and natural vegetation communities at continental scales (Justice *et al.* 1985).

These studies have shown that MVC imagery is highly related to green-vegetation dynamics, and that problems common to single-date remote-sensing studies, such as cloud contamination, atmospheric attenuation, surface directional reflectance, and view and illumination geometry, have been minimized. The following sections evaluate these influences on the basic assumption of the MVC technique, that of invariant cover-type stratification. The length of compositing period needed to minimize the influence of cloud cover, view angle and atmospheric effects is examined. Finally, conditions that limit the effectiveness of MVC are considered.

2. Evaluation of compositing

2.1. *Cover-type stratification*

Small-scale remotely sensed vegetation dynamics research with the NDVI requires that the magnitude of green vegetation be quantified to several levels and separated from other scene components such as clouds, bare soil, rocks and surface water. This is done by taking advantage of the stratification of cover classes as a function of the

Table 1. Stratification of the NDVI response to broad scene components as measured from NOAA-7.

Cover type	Planetary albedo		NDVI
	Channel 1	Channel 2	
Dense green-leaf vegetation	0·050	0·150	0·500
Medium green-leaf vegetation	0·080	0·110	0·140
Light green-leaf vegetation	0·100	0·120	0·090
Bare soil	0·269	0·283	0·025
Clouds (opaque)	0·227	0·228	0·002
Snow and ice	0·375	0·342	−0·046
Water	0·022	0·013	−0·257

NDVI. Average NDVI values, calculated from GAC VIS and NIR planetary albedos, for a variety of cover types, including oceans, lakes, sand deserts, grasslands, tropical rain forests, boreal forests, and ice caps, demonstrate this stratification (table 1). These data show a consistent stratification such that green vegetation has higher values than bare soil, which is higher than opaque clouds, which are higher than snow and ice, which are higher than water. These values are not intended to define an absolute range for each class, but rather to illustrate the consistent stratification of cover classes using the NDVI. The consistency of this stratification over time under a variety of atmospheric, viewing and illumination conditions, surface directional reflectance effects and cloud types determines the effectiveness of MVC.

Analysis of the potential impacts of atmospheric conditions and AVHRR viewing and illumination geometry on the NDVI stratification was conducted by simulating the NDVI using Dave's (1979) narrow-band simulations integrated to correspond to the NOAA-7 AVHRR VIS and NIR channels (Holben and Fraser 1984). Viewing geometry varied $\pm 56°$ from nadir, the solar zenith angle varied by 20° across a scan, and the solar azimuth changed by 10° to duplicate typical conditions observed by AVHRR. Three atmospheric compositions were included in the simulations: one corresponds to a Rayleigh atmosphere plus gaseous absorption; in the second, a nominal aerosol loading is added corresponding to a midlatitude continental condition, giving an effective aerosol optical thickness of 0·1; in the final model, the atmosphere is similar to the second, except that the aerosol optical thickness is raised to 0·5, a fivefold increase in the aerosol mass-loading. Lambertian surface reflectance was assumed for each scene component. The surface reflectance inputs for each cover class were based on average values from a variety of sources (table 2).

The cover-type stratification observed in the real AVHRR data (table 1) is also maintained in the simulated data over the $\pm 56°$ AVHRR scan, because the NIR and VIS channel responses change approximately proportionally as cosine functions of viewing and illumination geometry (Holben and Fraser 1984) (figure 1). The simulations show the NDVI for any cover type to be a maximum near the nadir slightly in the forward-scattering direction and decrease with off-nadir viewing for all cover types but water. Clear water has a low reflectance in the NIR band (0·5 per cent), which results in an NDVI very much lower than other cover types under identical conditions.

Under a constant atmospheric condition the influence on the stratification is unchanged (figure 1). As the aerosols are increased, all cover-type NDVIs are reduced

Table 2. Input surface reflectances for the Dave simulations of various general classes of targets.

Class	Reflectance		Comment
	VIS	NIR	
High green-leaf-vegetation density	0·03	0·40	Kimes *et al.* (1984 a), closed canopy
Moderate green-leaf-vegetation density	0·05	0·25	Kimes *et al.* (1984 b), 50 per cent canopy cover
Low green-leaf-vegetation density	0·10	0·20	Author's observations
Bare soil	0·20	0·25	Author's observations
Opaque clouds	0·60	0·60	Author's observations
Water	0·005	0·00	Author's estimate

except clear water. The cover-type stratification is maintained because the clear-water values are lower than the minimum values of the other cover types.

The influence of surface directional reflectance was examined by passing measured surface directional reflectance of three cover classes including bare soil and two levels of green vegetation (Kimes *et al.* 1984a) through Dave's (1979) atmospheric models. The Dave models were adapted to accept directional reflectance (Holben *et al.* 1986), which enabled simulations for the same atmospheric conditions previously described. The results show that directional-reflectance effects maintain the stratification for the cover types simulated for all view angles (Holben *et al.* 1986). These simulations indicate that surface directional reflectance does not affect the NDVI, principally because the reflectance properties that influence nadir viewing operate similarly for off-nadir viewing. Quantitative directional-reflectance studies have not been made over water and opaque clouds in the AVHRR visible and NIR bands; however, observational data, which include off-nadir measurements from the NOAA-7 AVHRR, indicate that the stratification is maintained over opaque clouds and ocean water (tables 1 and 2).

2.2. *Processing multitemporal NDVI images into an MVC image*

Maintenance of the cover stratification is fundamental to MVC. The NDVI values for all cover types increase with lower aerosol concentrations, near-nadir viewing and high Sun illumination. Hence the concept of MVC assumes that any attenuation of the spectral signals will reduce the NDVI value from that of an unattenuated signal. Therefore, the best possible pixel value for a particular location is achieved by choosing the highest pixel value from multitemporal data.

2.2.1. *Viewing and illumination*

The previous subsections have demonstrated that the cover-type stratification was maintained under varying viewing and illumination conditions. Additionally, the same data (figure 1) show that the NDVI is a maximum for each cover type for near-nadir viewing and small solar zenith angles. As mentioned earlier, clear surface water has values at a maximum in the extreme view directions owing to path radiance; however, because the maximum clear-water NDVIs are well below the minimums of other cover

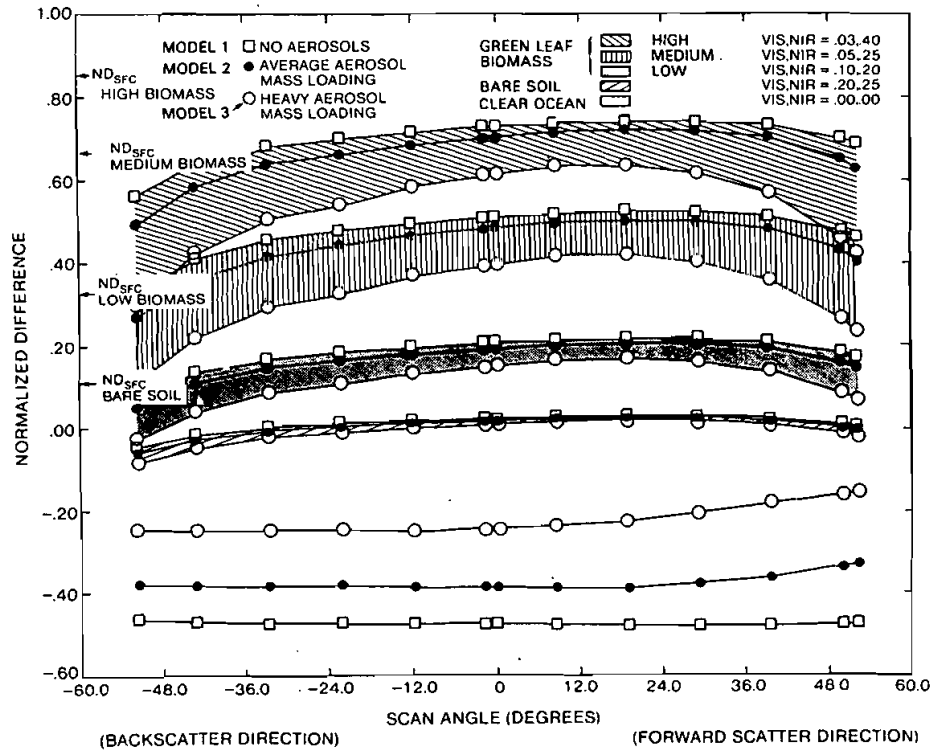

Figure 1. The NDVI was simulated as a function of NOAA-7 and 9 viewing and illumination geometry during the summer solstice for green vegetation, bare soil and water.

types, an MVC image for vegetation analysis remains unaffected. The viewing geometry selected through MVC is such that near-nadir-viewed pixels (nadir to + 10°) will usually be chosen. This will shorten the viewing slant path, which necessarily reduces the influence of the atmosphere on the signal and minimizes surface directional effects, which can be substantial for green vegetation (Kimes *et al.* 1984a, Kriebel 1978).

Illumination geometry plays an important role in determining the NDVI. The solar zenith angle varies by 20° along an AVHRR scan line at 30° latitude and by a maximum of 47·0° owing to seasonal changes. The response of the NDVI to illumination geometry was shown by contrasting the Dave simulations for a hazy atmosphere at a solar zenith 34° and 64°. These angles correspond to NOAA-7 and 9 passes at the summer and winter solstices respectively. Figure 2 shows a decrease in the NDVI relative to figure 1 for each of the three cover types owing to a larger solar zenith angle. It should be noted that this apparent response to the solar zenith angle also includes the effect of solar azimuth, accounting for the total effect of illumination geometry. These simulations suggest that composite multitemporal imagery is comprised of data having the smallest solar zenith angles, thereby minimizing shadows, which lower the NDVI values.

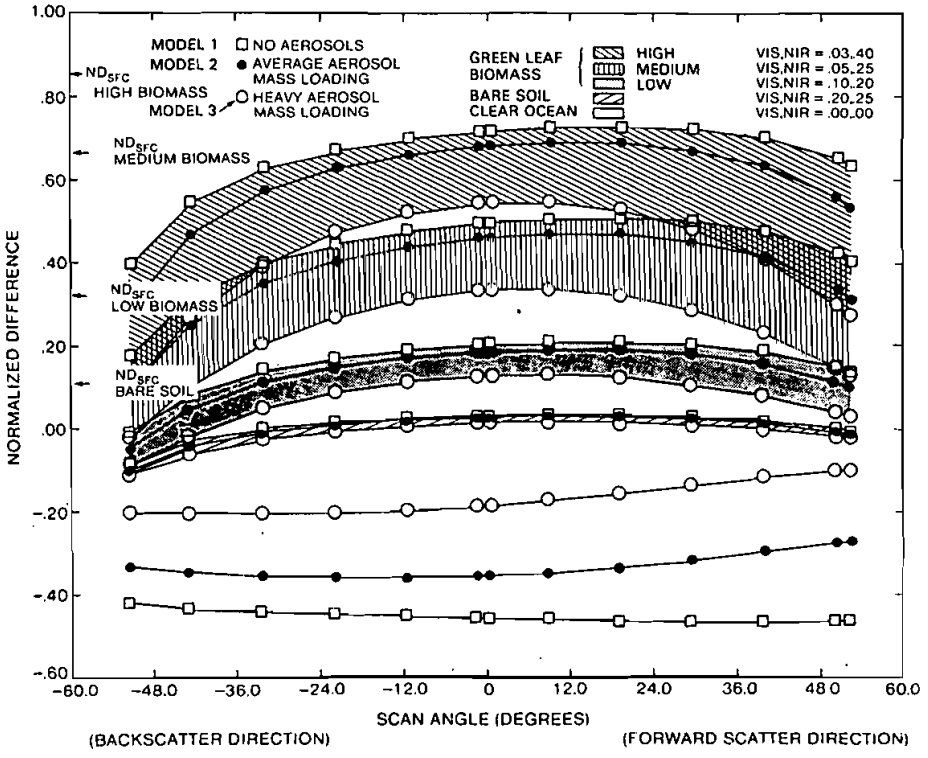

Figure 2. The NDVI was simulated for AVHRR viewing and illumination conditions of NOAA-7 and 9, i.e. 1430 (local time) equatorial crossing during the winter solstice (solar zenith angle 64°) for cover types.

2.2.2. *Atmospheric constituents*

The constituents of a cloudless atmosphere may affect the signal by scattering and/or absorption. Scattering can either increase or decrease the channel signal, whereas absorption can only decrease the signal. The NDVI can either increase or decrease in value, depending on the magnitude of the attenuation in each channel. The following is a discussion of the atmospheric constituents that affect the composite image process.

The constituents in a cloudless atmosphere that affect AVHRR NDVI data are air molecules, which cause Rayleigh scattering, oxygen, ozone, other trace gases and water vapour, which cause absorption, and aerosols, which cause both scattering and absorption. Rayleigh scattering is nearly invariant over time, as the number of molecules in a column of atmosphere is nearly constant; thus the NDVI will be little affected over time and space. Oxygen absorption is very weak in the near-infrared band, depending on the surface air pressure (McClatchey *et al.* 1972). The result is to decrease NDVI values by less than one per cent under normal pressure fluctuations. This decrease in NDVI values would be minimized in a MVC image, so that it is well within the noise of other causes of variation of the NDVI. The ozone Chappuis band (0·55–0·64 μm) results in weak absorption in the visible band, and is expected to increase the NDVI. Ozone concentrations occurring naturally in the atmosphere range

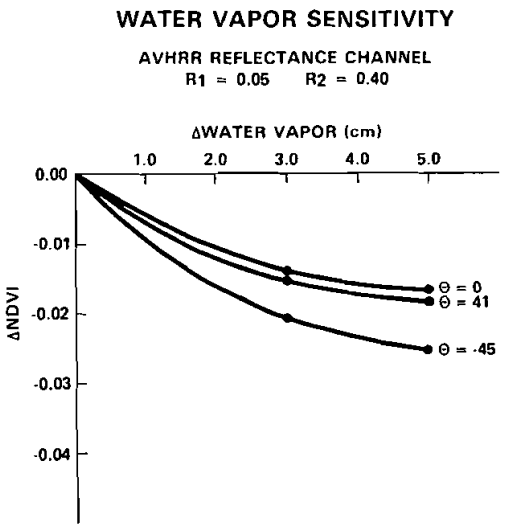

Figure 3. The change in NDVI was simulated as a function of precipitable water for three viewing angles of NOAA-7 and 9 AVHRR for a dense green-leaf canopy during the summer solstice.

from 0·24 to 0·44 atm-cm (London *et al.* 1976), being highest in polar regions during the spring. NDVI corrections for ozone are relatively straightforward, as attenuation of the NDVI is relatively small, and concentrations over time and space are well known.

Water vapour and aerosols are highly variable over time and space, as such causing the greatest variation in atmospherically attenuated AVHRR short-wave data. Water vapour in the atmosphere decreases the NIR channel response, which is shown to be approximately eight per cent of the signal response, assuming complete absorption. Several water-vapour concentrations were chosen to represent realistic atmospheric conditions, the radiances modelled and the percentage change in reflectance and NDVI plotted against the per cent change in precipitable water (figure 3). These simulations show that the overall effect of water vapour is to decrease the NIR surface reflectance by 3–5 per cent for common ranges of precipitable water (2–4 cm), thereby decreasing the NDVI by 0·02 units. These values are not large and are further reduced by MVC. Water vapour would have no influence on the cover-type stratification.

As in the water-vapour case, aerosols lower the NDVI without altering the stratification of the cover classes. This result is evident from two examples. In the first example, simulations from the Dave radiation transfer models show that a change in optical thickness owing to aerosols from 0·1 to 0·5 decreased the NDVI by 0·12 units in the extreme-backscatter direction and by 0·06 units in the nadir (figure 4). The second example is a simulation of the satellite level NDVI for the cover types under varying levels of atmospheric aerosol concentrations. The simulations show that extreme off-nadir viewing reduces the NDVI of all classes except water, and that soil and vegetation classes always have higher NDVI values than water or clouds for a particular viewing and atmospheric composition (figures 1 and 2). Therefore the MVC technique will result in image values that correspond to the lowest aerosol concentrations, other variables being constant.

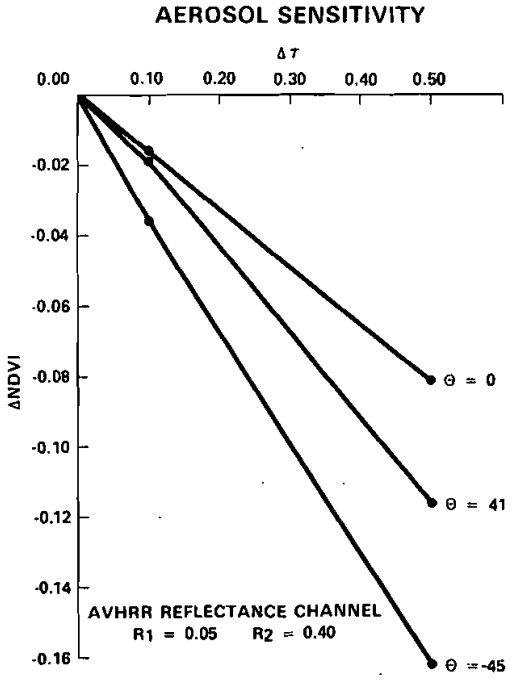

Figure 4. The change in NDVI was simulated as a function of aerosol optical thickness for three viewing angles of NOAA-7 and 9 AVHRR for a dense green-leaf canopy during the summer solstice.

2.2.3. *Directional surface reflectance*

The response of a satellite sensor to directional surface reflectance is dependent on both the viewing and illumination geometry. In the case of the AVHRR, the illumination geometry changes as the satellite scans East–West. Small changes in illumination geometry occur in MVC data sets, owing to seasonal changes in solar zenith and azimuth angles, but are unimportant relative to variations caused by viewing across many degrees of longitude. The simulations illustrate that the NDVI values are reduced slightly with increasing view angle, but are unimportant relative to the atmospheric sources of variation described here (figure 5).

2.2.4. *Temporal data for MVC imagery*

The best possible NDVI MVC image is produced under clear atmospheric conditions, high Sun conditions, low water vapour and near-nadir viewing for each pixel. These conditions cannot be met without selecting pixels from a large number of contiguous temporal images. The number of scenes needed can be computed with a knowledge of the probabilities of occurrence of each of the above components for specifically acceptable limits of remote sensing.

The following example is a simple illustration of the temporal data needed for MVC under specific conditions. Assume that the probability of a cloud-free day is 0·20 and a cloudy day is 0·80, the probability of a haze-free day is 0·20 and a hazy day is 0·80, and finally that the probability of a nadir value is 0·33 and an off-nadir value is 0·67. Assume also that the satellite views only clouds and low-density green vegetation and that nadir observation of clouds returns a higher NDVI value than off-nadir hazy low-

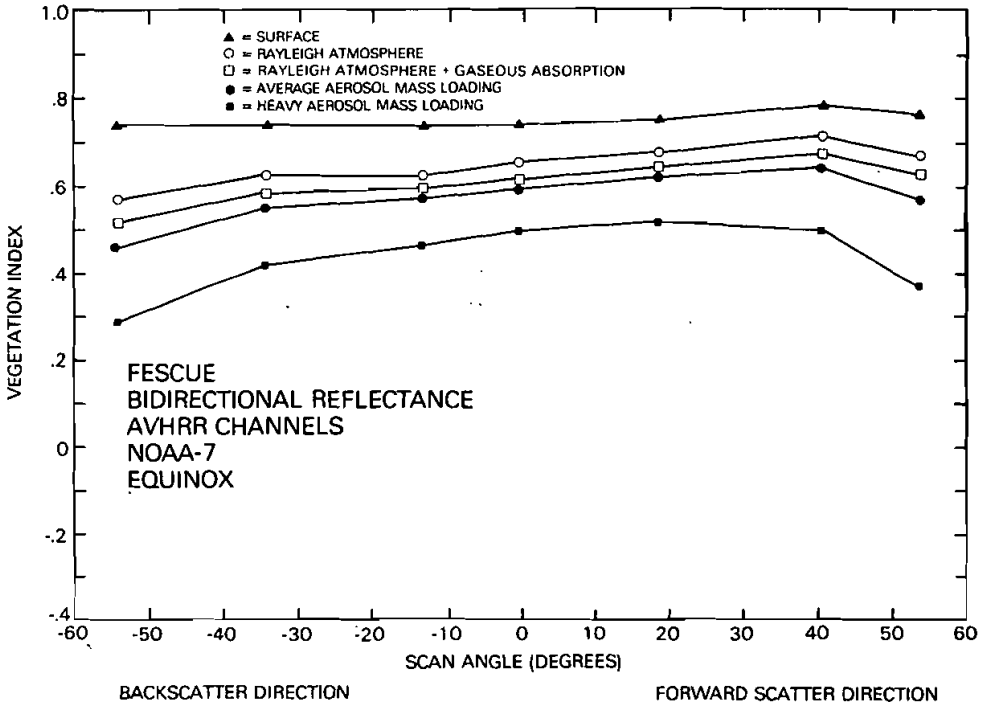

Figure 5. The NOAA-7 and 9 AVHRR NDVI was simulated from measured surface directional reflectances for four atmospheric conditions at equinox viewing and illumination conditions and plotted as a function of scan angle.

density green leaf vegetation. The probability conditions are listed in table 3, and the probability combinations are presented in table 4. Four out of five observations will be cloudy (sum of probabilities for ranks 4, 6, 7, 8, table 4); therefore, five observations are expected to produce a NDVI image of vegetation via MVC. One in eleven observations (sum of ranks 1, 2, 3, table 4) is expected to obtain a NDVI value higher than that returned from a cloud (rank 5, table 4). To obtain the highest NDVI under these conditions, one observation in 77 (rank 1, table 4) is needed to produce a cloud-free haze-free NDVI image.

This example illustrates that MVC can be used to produce imagery of areas normally difficult to monitor with passive systems owing to climatic factors with the daily global GAC coverage by the AVHRR. Furthermore, most cloud contamination can be detected and masked out of the MVC images using a thermal threshold based on the AVHRR channel 4 temperatures (10·5–11·5 μm) (Gatlin *et al.* 1984).

These observations were further corroborated by evaluating an eight-day MVC scene of Africa using its daily scenes (figure 6). The daily longitudinal progression of the satellite is from West to East by three degrees. The scene is viewed off-nadir in the forward-scatter direction. A boxed portion of the Angolian highlands is used as a reference. A daily progression of the NDVI is apparent as being low in the backscatter direction (16, 17 August), higher in the nadir while lower in the forward-scatter view (22, 23 August). Equatorial Africa is very cloud contaminated on the daily images (figures 6 (*a*) and (*b*)), as evidenced by dark patches resulting from the thermal cloud mask. The MVC image (figure 6 (*c*)) has very high values (light-toned) in the equatorial

Table 3. The probability of occurrence of six conditions affecting AVHRR monitoring of the Earth's surface.

Hazy (HZ)	Non-hazy (NHZ)	Nadir (N)	Off-nadir (O-N)	Cloudy (CLDY)	Non-cloudy (CLR)
0·80	0·20	0·33	0·67	0·80	0·20

Table 4. The probability of occurrence of eight possible combinations ranked according to NDVI.

Combination†	Probability	Rank
N, CLR, NHZ	0·013	1
N, CLR, HZ	0·053	2
O-N, CLR, NHZ	0·026	3
N, CLDY, HZ	0·053	4
O-N, CLR, HZ	0·107	5
N, CLDY, NHZ	0·211	6
O-N, CLDY, NHZ	0·107	7
O-N, CLDY, NHZ	0·429	8

†For nomenclature see table 3.

region, indicating that cloud contamination has been reduced. The maximum NDVI value occurs for the middle dates when view angles are smaller, thereby reducing attenuation from the atmosphere (figure 6 (*d*)). Longer compositing periods may be used to further minimize these errors.

Besides the optical properties of the target and atmosphere, the vegetation dynamics to be monitored govern the time interval over which to produce MVC images. The previous discussion establishes that longer MVC time intervals are advantageous for reducing the influence of these factors. The accuracy for characterizing response curves such as photosynthetic activity during a growing season improves as the number of quantizing intervals becomes smaller. An *a priori* knowledge of the phenological response curve of a particular cover type and the quality of the information desired would be the best guide for setting a maximum acceptable limit to the time interval for generation of an MVC image. For example, to capture the green-wave response curve of the approximately six week arctic tundra growing season requires relatively short MVC quantizing intervals. In contrast, the longer-term response curve of a tropical evergreen forest having an eight-month active growing season can be monitored with longer MVC quantizing intervals.

2.3. *Problems associated with MVC*

The MVC technique has been shown to minimize significant problems associated with short-wave passive remote sensing of the Earth's surface. The MVC technique

Figure 6. The NDVI composite-image technique selects the maximum value on a pixel-by-pixel basis from a series of single-date images. In these figures lighter tones represent higher values. Referencing the black box over Angola, NDVI values at the extreme view angles (*a*) and (*b*) are lower than the composite image (*c*). The daily progression of values shows that highest values occur for the middle dates, i.e. when viewing near nadir (*d*).

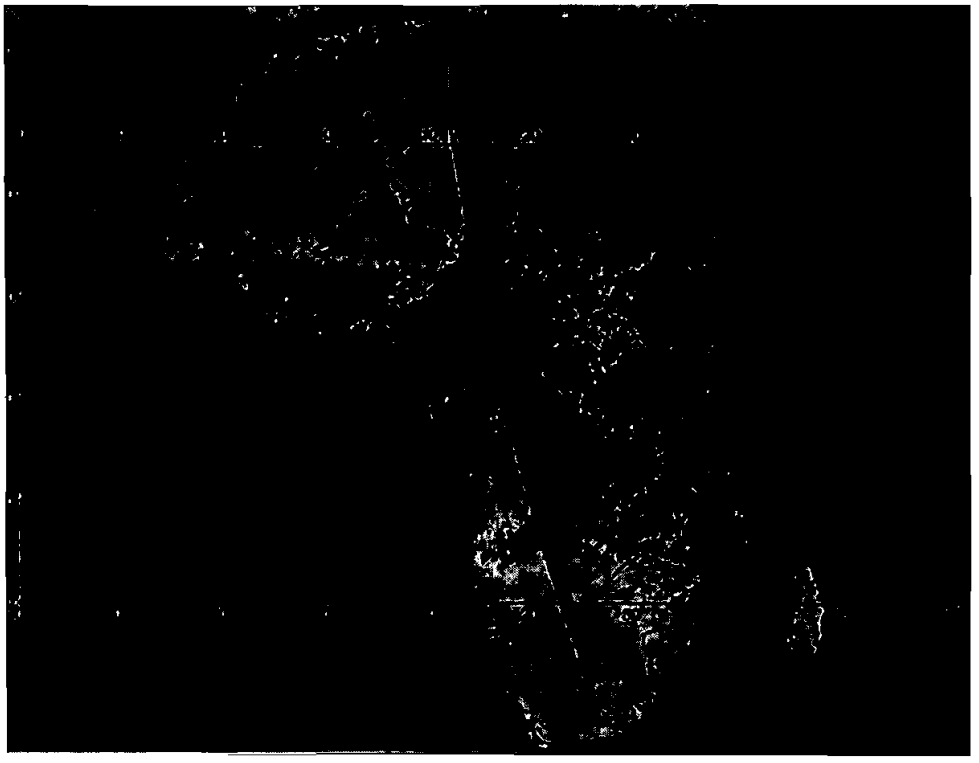

(*a*)

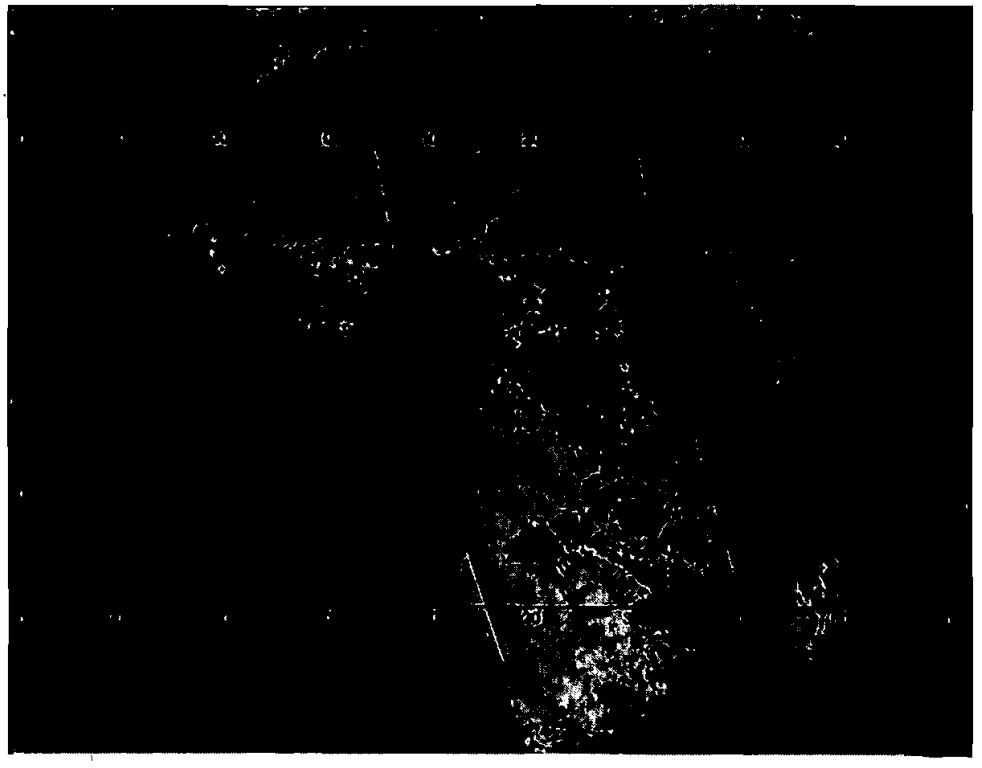

(*b*)

Figure 6.

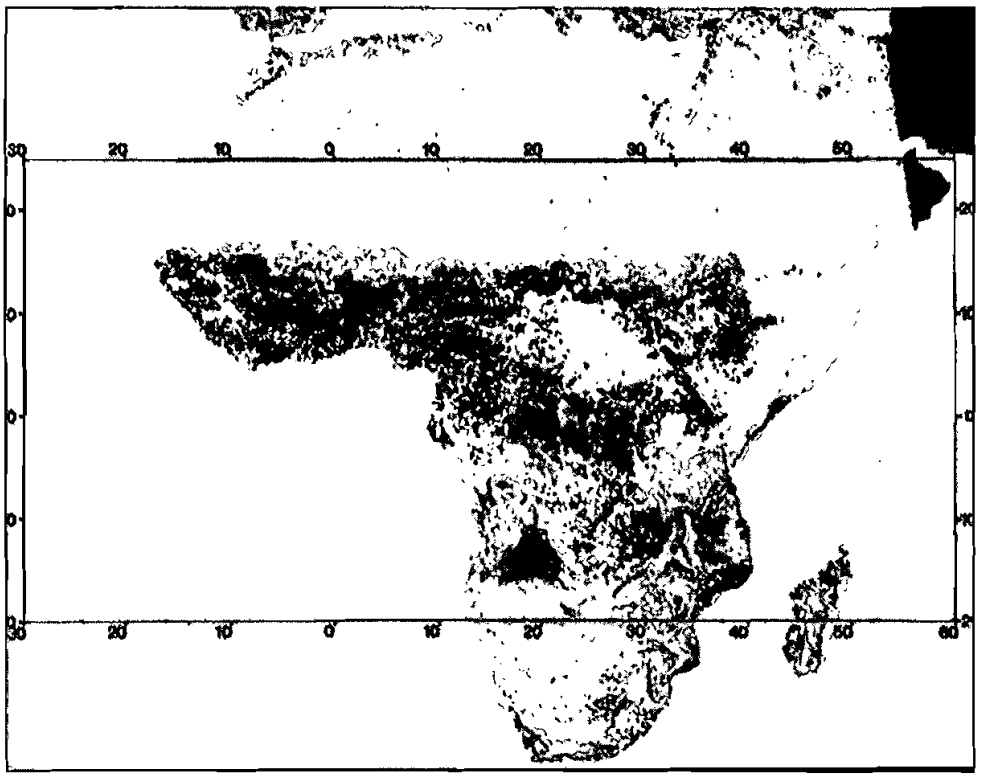

Figure 6 (c).

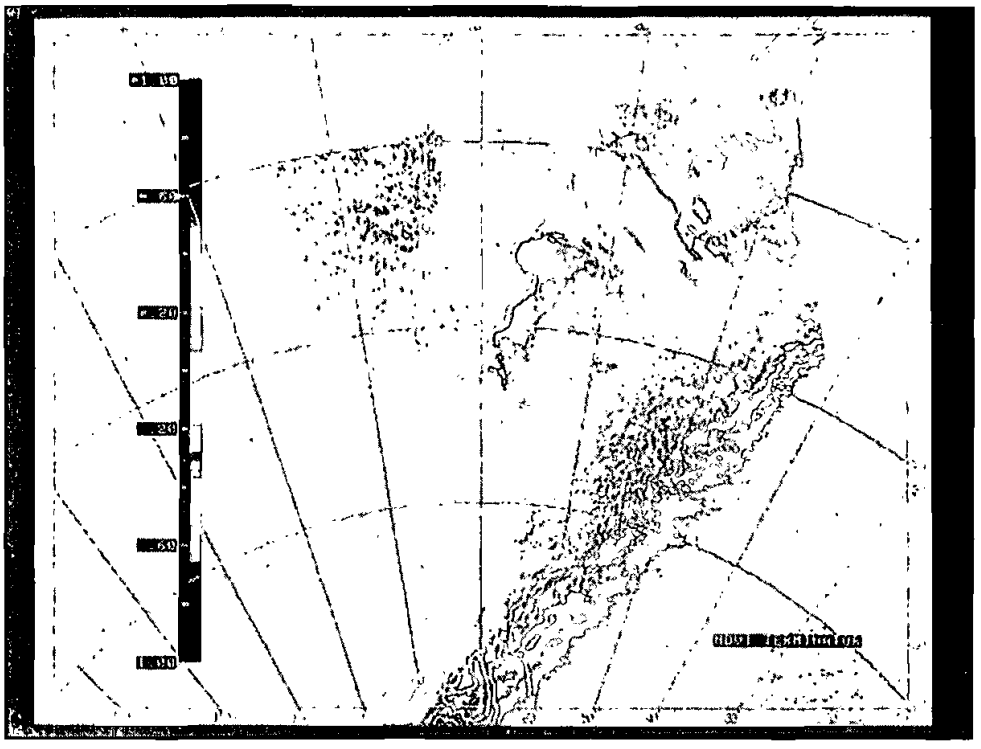

Figure 7. An NDVI image showing highest values near the terminator.

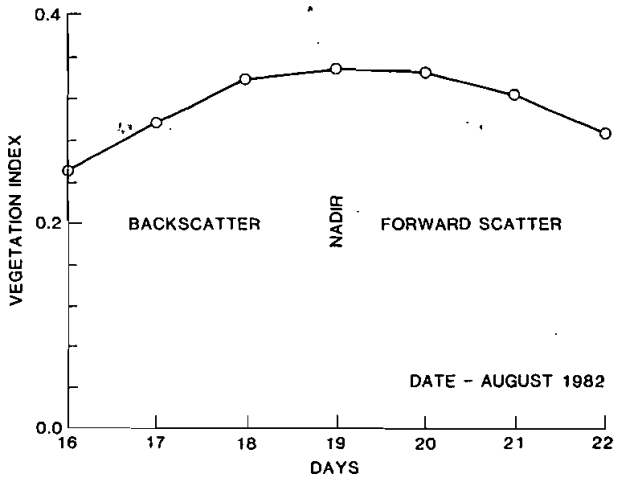

Figure 6 (*d*)

itself has generated a second level of problems that must be addressed for proper interpretation of the NDVI MVC images. These are radiometric effects, which are relevant to the stratification assumption, and engineering effects, which are relevant to the MVC technique. In the first instance we evaluate the basic assumption of cover-type stratification as influenced by subpixel-sized clouds, the assumption of constant NDVI for bare soil, and the influence of very low radiance values causing highly variable NDVI values. Finally, the engineering controlled Earth location data may in some cases reduce the spatial resolution of MVC images.

2.3.1. *Cloud contamination*

The stratification assumption can be altered by clouds of variable thickness, particularly thin cirrus; specular reflection from oceans; low light levels near the terminator, and low reflectance responses of scene components within mixed pixels as might occur in desert salt pans or green vegetation growing over water. Of the above, clouds of variable transparency will most commonly alter the stratification scheme. This is due to mixed cover-type response applied to a rigid cover-type response scheme. For example, if a thin nearly transparent cirrus cloud obscures a clear view of a vegetated surface then the resulting NDVI response may be that of a partially vegetated surface. If the cloud-mask procedure detects a cloud at a pixel location, no NDVI data are available for the MVC selection process. The thermal mask is useful for detecting cold clouds such as thin cirrus and cumulus, and the visible mask is useful for warm low-level clouds. The cloud mask also enables production of cloud-free imagery over water bodies using MVC.

Six procedures using VIS and thermal infrared (IR) for cloud screening were evaluated by Nixon *et al.* (1982). They found that both visible and thermal IR thresholding were less effective than thresholding a ratio of the VIS to thermal IR. This latter procedure worked well because clouds are the brightest scene components in the reflective channel (excluding snow), and they are usually colder than land features in the emissive bands. Therefore VIS/thermal-IR ratios contrasted clouds very well

versus other scene components. The most successful techniques took advantage of clustering of surface features under clear sky conditions and dispersion of cloud-contaminated data.

2.3.2. *Desert anomalies*

There are several situations in which MVC does not operate successfully owing to a breakdown of the stratification assumption. One such case occurs in less than 10 per cent of the Sahara desert on a quasi-permanent basis. NDVI values taken on individual dates across the Sahara show that MVC does not operate successfully owing to a breakdown of the stratification assumption. These NDVI values are associated with increased NIR values and little change in the VIS channel (table 5). Furthermore, vegetated areas of sub-Saharan Africa show increases in the NDVI associated with slight decreases in the NIR channel, and larger decreases in the VIS channel, contrary to the normally expected responses of higher NDVI driven by higher NIR radiances. Spectral observations of bare soil and green vegetation indicate the reflectance in the visible portion of the spectrum to be low for soil, lower for green vegetation; in the NIR, relatively higher for bare soil, higher still for green vegetation (Stoner *et al.* 1979, Gates, *et al.* 1965, and many others). These studies support the stratification concept of MVC, but run counter to some of the AVHRR observations.

An evaluation is beyond the scope of this paper; however, it may be speculated that a combination of factors is influencing this observed response. Assuming that, owing to the broad bandwidth of the AVHRR VIS and NIR channels, their nearly equal response represents their nominal condition over the Sahara, then the soil (sand) mineralogy, combined with soil structure, is causing an increase in the AVHRR NIR response. Secondly, Stoner *et al.* (1979) report that a decrease in soil moisture increases soil reflectance for all wavelengths. Their data show in particular that sandy soils have a disproportionately higher increase in the NIR than finer textured soils. This, combined with low precipitable water in the atmosphere (assuming that there is a positive correlation with soil moisture), would also cause an increase in the NIR. This may begin to explain the higher NDVI response over non-vegetated areas and the quasi-permanent nature of some of the features observed in the AVHRR imagery. Further research is needed to fully determine the spatial and temporal range of the NDVI, VIS and NIR values over non-vegetated and partially vegetated areas.

Table 5. VIS and NIR counts and NDVI values for bare soil and green vegetation as measured at selected sites over the Sahara and Sahel with NOAA-7 AVHRR on 18 August 1984.

	VIS	NIR	NDVI
Nominal	217	210	−0·018
bare-soil values	231	230	−0·004
	206	209	0·006
Anomalous	246	290	0·070
bare-soil values	225	260	0·074
	232	272	0·078
	232	275	0·084
Low	157	202	0·125
green-vegetation density	180	210	0·076
Moderate green-vegetation density	121	214	0·277

Table 6. NDVI, VIS and NIR planetary albedo count values and solar zenith angles taken at selected sites along the terminator area.

Location/description/target	NDVI	VIS	NIR	
		Counts		%
1. Near nadir/dark/clouds, ice	0·109	4	5	94·0°
2. Forward/terminator/clouds, ice	0·285	5	9	92·1°
4. Forward/terminator/clouds, ice	0·230	5	8	91·3°
5. Forward/terminator/clouds	0·172	12	17	87·5°
7. Near nadir/daylight-terminator clouds	0·094	38	46	82·1°
9. Forward/daylight/clouds	0·018	138	143	76·9°
11. Nadir/daylight/water	−0·174	17	12	72·3°

2.3.3. *Terminator effect*

The stratification assumption does not hold at high latitudes near the twilight terminator. High NDVI values occurring in a band along the terminator are generated in response to very long path lengths, which are largely independent of the surface reflectance. Similar spurious values result from NDVI values calculated at night.

A winter image of South America and Antarctica demonstrates a very pronounced NDVI terminator response, with high values extending from the Antarctic continent at 70° S latitude and 70° W longitude extending to the NE over the south Atlantic at 45° S and 42° W (figure 7). Values ranged from 0·172 to 0·285 along the main core of the NDVI terminator, decreasing to 0·109 in the dark area south of the terminator and 0·094 in the daylight area north of the terminator (table 6). These data show that the NDVI terminator response is most pronounced when the scanner is looking towards the forward-scatter direction. More importantly, these data show that high NDVI values are associated with very low VIS and NIR values owing to solar zenith angles greater than 80° (table 6). Finally, it is apparent that the NDVI terminator response is independent of the surface reflectance, manifested as a continuous band over bright surfaces, such as cloud and snow, and dark surfaces, such as water.

Therefore, the NDVI terminator response is a result of atmospheric scattering and absorption at very large solar zenith angles. The evidence shows that the NDVI terminator response occurs when the ground radiance is negligible. Since it follows that no AVHRR MVC data sets with solar zenith angles greater than 80° contain information on surface properties, they should be eliminated, for example, by thresholding the solar zenith angle. Further research is continuing on the characteristics of the NDVI terminator response and the limits of the solar zenith angle thresholding as a function of atmospheric composition, view angle and solar azimuth angle.

2.3.4. *Registration*

The MVC technique is affected by spatial misregistration of multitemporal data. Data used for composite multitemporal images are mapped to exactly the same projection variables. This registration of the mapped imagery is dependent on the accuracy of the location information imbedded in the AVHRR data. The location information varies depending on the source of the AVHRR data. The University of Miami, under contract from the Department of Defense, developed software to locate

Table 7. Across track and along track registration shifts.

Date	Across track (km) East (+) west (−)	Along track (km) North (+) south (−)	Control points used	Date	Across track (km) East (+) west (−)	Along track (km) North (+) south (−)	Control points used
2 May	1·2	4·4	2	22 July	7·0	−5·2	4
3 May	2·3	8·1	2	23 July	4·7	−5·9	3
4 May	3·5	8·9	3	24 July	7·0	−4·4	2
10 May	3·5	4·4	2	29 July	7·0	−3·7	1
11 May	2·3	5·2	2	30 July	8·2	−4·4	5
12 May	7·0	8·9	4	15 August	3·5	0·0	4
18 May	2·3	7·4	3	1 September	4·7	−2·2	4
19 May	2·3	5·2	4	9 September	4·7	−1·5	4
27 May	−1·2	8·9	3	17 September	4·7	0·0	4
28 May	0·0	8·1	3	30 September	4·7	−3·0	4
11 June	1·2	10·4	4	15 November	4·7	−3·0	4
12 June	1·2	7·4	3	22 November	4·7	−2·2	2
19 June	2·3	6·7	5	24 November	4·7	−0·7	2
30 June	2·3	8·1	1	25 November	4·7	−0·7	2
5 July	0·0	8·9	5	8 December	2·3	0·0	3
7 July	2·3	11·1	2	9 December	2·3	2·2	4
14 July	0·0	−3·0	4	17 December	3·5	3·0	3
15 July	4·7	−3·7	4	18 December	3·5	2·2	1
16 July	4·7	−5·2	2				
Absolute mean			3·6 km			4·8 km	
Range			8·2→−1·2			11·1→−5·9	

LAC data within +1 km in the nadir (O. Brown 1984 personal communication). NOAA has this software, but is not scheduled to implement it on commercially available AVHRR tapes until 1986 (J. Ellickson 1984 personal communication). NOAA nominally specifies their navigation to ±5 LAC pixels at the satellite subpoint.

The current NOAA location data can have two sources of error: along track and across track. Along-track errors are primarily caused by inaccuracies in knowing the true time of the onboard tracking clock and, to a lesser extent, by the effects of satellite pitch. The second error is caused by inaccuracies in compensating for yaw and roll.

Thirty LAC images of East Africa, corresponding to similar viewing conditions, were selected between 2 May 1983 and 18 December 1983. The images were mapped according to identical projection variables and then registered according to eight control points located at the tip of peninsulas along Lakes Turkana, Victoria and Tanganyka as measured on Operational Navigation Chart M5. This choice was made because these lakes induce atmospheric subsidence over themselves and adjacent land during times of NOAA-7 overpasses, resulting in relatively cloud-free imagery over the registration points. These data showed that the mean along-track error is approximately 4·8 km and across-track error is 3·6 km (table 7). Extreme cases in this data set have shown that the along-track misregistration can vary by as much as 17 km.

Misregistration affects MVC by assigning high NDVI values to adjacent areas of lower NDVI. For very large uniform areas, misregistration is of little importance, but for small-scale AVHRR studies in areas of contrasting NDVI values such as water/green-vegetation boundaries, misregistration can become a significant problem. Control-point registration of LAC data is recommended until NOAA is able to implement improved location software.

The measured LAC registration is approximately the size of one GAC pixel, which was verified by a similar procedure using GAC pixels. This error, albeit small for most GAC-scale studies, should be considered for GAC investigations. Studies involving degraded GAC spatial resolution are not greatly affected by the registration problem.

3. Conclusions

Two assumptions of the MVC technique have been shown to be valid under a variety of remote-sensing conditions. First, cover-type stratification is maintained for a large range of viewing and illumination conditions and for all aerosol conditions; other atmospheric constituents were also shown not to affect the stratification. Secondly, the maximum value of the NDVI for a particular cover type was demonstrated to occur consistently when viewing near nadir and at small solar zenith angles, thus minimizing any response caused by directional reflectance from the surface. These phenomena, combined with a thermal or visible cloud mask, result in suitable images for monitoring green-vegetation dynamics using temporal AVHRR data.

These simulations indicate that the degree of influence of clouds, sun angle, water vapour, aerosols and directional surface reflectance is minimized in MVC NDVI imagery as the length of the quantizing interval is increased. In contrast, the quantizing interval must be determined by the amplitude and period of the response curve of the vegetation to be monitored: for example, a very large quantizing interval may less accurately approximate the response curve of the green vegetation. Therefore a trade-off must be made in determining the optimum length of time for the quantizing interval based on an *a priori* knowledge of the response curve. Successful MVC processing of multitemporal imagery requires a base accuracy of registration commensurate with the spatial resolution of the individual images: poor spatial registration can improperly shift the location of NDVI boundaries, thereby artificially reducing the area of low NDVIs. The present author, having evaluated NOAA registration for LAC and GAC data, given the existing NOAA processing, has found registration necessary for multitemporal LAC analysis; therefore, registration should be a consideration for GAC resolution studies. Degraded GAC imagery of 8 km or more does not benefit from interactive registration.

Acknowledgments

I wish to thank Jim Gatlin for the African figures, Chris Justice, Jim Tucker, Jean-Paul Malingreau, Sam Goward and Tom Goff for their reviews and comments, and Bob Fraser for his assistance with the atmospheric modelling.

References

DAVE, J. V., 1979, Extensive data sets of the diffuse radiation in realistic atmospheric models with aerosols and common absorbing gases. *Sol. Energy*, **21**, 361.

DEERING, D. W., ROUSE, J. W., HAAS, R. H., and SCHALL, J. A., 1975, Measuring Forage Production of Grazing Units from Landsat MSS data. *Proceedings of the 10th International Symposium on Remote Sensing of the Environment*, Ann Arbor, Michigan, p. 1169.

GATES, D. M., KEEGAN, H. J., SCHLETER, J. C., and WEIDNER, V. R., 1965, Spectral properties of plants. *Appl. Optics*, **4**, 11.

GATLIN, J. A., SULLIVAN, R. J., and TUCKER, C. J., 1984, Monitoring global vegetation using NOAA-7 AVHRR data. *Proceedings of the 1983 International Geoscience and Remote Sensing Symposium*, San Francisco, California, PF2, 7.1.

GATLIN, J. A., TUCKER, C. J., and SCHNEIDER, S. R., 1981, Use of NOAA-6 AVHRR channels one and two for monitoring vegetation. *Proceedings of the 1981 International Geoscience and Remote Sensing Symposium*, Institute of Electrical Engineers, New York, abstract, p. 454.

GOWARD, S. N., TUCKER, C. J., and DYE, D. G., 1985, North American vegetation patterns observed by the NOAA-7 AVHRR. *Vegetation*, **64**, 3.

GRAY, T. I., and MCCRARY, D. C., 1981, Meteorological satellite data—A tool to describe the health of the World's agriculture. AgRISTARS Report EW-NI-04042, JSC, Houston, Texas.

HOLBEN, B. N., and FRASER, R. S., 1984, Red and near-infrared sensor response to off-nadir viewing. *Int. J. remote Sensing*, **5**, 160.

HOLBEN, B. N., KIMES, D., and FRASER, R. S., 1986, Directional reflectance response in AVHRR red and near-infrared bands for three cover types and varying atmospheric conditions. *Remote Sensing Environ.* **19**, 213.

JUSTICE, C. O., HOLBEN, B. N., and GWYNNE, M. D., 1986, Monitoring East African vegetation using AVHRR data. *Int. J. remote Sensing*, **7**, 1453.

JUSTICE, C. O., TOWNSHEND, J. R. G., HOLBEN, B. N., and TUCKER, C. J., 1985, Phenology of global vegetation using meteorological satellite data. *Int. J. remote Sensing*, **6**, 1271.

KIDWELL, K. B., 1984, NOAA polar orbital data user's guide (TIROS-N, NOAA 6, 7, 8). NOAA National Climate Center, Washington, D.C.

KIMES, D. S., HOLBEN, B. N., TUCKER, C. J., and NEWCOMB, W. W., 1984 a, Optimal directional view angles for remote sensing missions. *Int. J. remote Sensing*, **5**, 887.

KIMES, D. S., NEWCOMB, W. W., TUCKER, C. J., ZONNEVELD, I. S., VAN WIJNGAARDEN, W., DE LEEUW, J., and EPEMA, G. F., 1984 b, Directional reflectance factor distributions for cover types of northern Africa in NOAA 7/8 AVHRR bands 1 and 2. *Remote Sensing Environ.*, **18**, 1.

KRIEBEL, K. T., 1978, Measured spectral bidirectional reflection properties of four vegetated surfaces. *Appl. Optics*, **17**, 253.

LONDON, J., BOJKOV, R. D., OLTMANS, S., and KELLEY, J. I., 1976, Atlas of the global distribution of total ozone, July 1957–June 1967. NCAR/TN/113+STR, Boulder, Colorado.

MCCLATCHEY, R. A., FENN, R. W., SELBY, J. E. A., VOLZ, F. E., and GARING, J. S., 1972, Optical properties of the atmosphere. AFCRL-72-0497, Hanscom Field, Bedford, Massachusetts.

NIXON, P. R. WIEGAND, C. L., RICHARDSON, A. J., and JOHNSON, M. P., 1982, Methods of editing cloud and atmospheric layer affected pixels from satellite data. Final Report NASA-CR-169679, Code 601 GSFC, Greenbelt, Maryland.

NOAA, 1983, Global vegetation index user's guide. SDS/NESDIS, National Climate Data Center, Washington, D.C.

SCHNEIDER, S. R., and MCGINNIS, D. F., JR., 1982, The NOAA AVHRR: A new sensor for monitoring crop growth. *Proceedings of Machine Processing of Remotely Sensed Data Symposium*, LARS, West Lafayette.Indiana, p. 281.

SELLERS, P. J., 1985, Canopy reflectance, photosynthesis and transpiration. *Int. J. remote Sensing*, **6**, 1335.

STONER, E. R., BAUMGARDNER, M. F., BIEHL, L. L., and ROBINSON, B. F., 1979, Atlas of soil reflectance properties. Purdue University, West Lafayette, Indiana, LARS Technical Report 111579.

TARPLEY, J. P., SCHNEIDER, S. R., and MONEY, R. L., 1984, Global vegetation indices from NOAA-7 meteorological satellite. *J. Climate appl. Meteorol.*, **23**, 491.

TOWNSHEND, J. R. G., and JUSTICE, C. O., 1986. Analysis of the dynamics of African vegetation using the normalized difference vegetation index. *Int. J. remote Sensing*, **7**, 1435.

TOWNSHEND, J. R. G., and TUCKER, C. J., 1981, Utility of AVHRR of NOAA 6 and 7 for Vegetation Monitoring. *Proceedings of Matching Remote Sensing Technologies and Their Applications* (Reading, England: Remote Sensing Society).

TUCKER, C. J., GATLIN, J., SCHNEIDER, S. R., and KUCHINOS, M. A., 1982, Monitoring large scale vegetation dynamics in the Nile Delta and River Valley from NOAA AVHRR data. *Proceedings of Conference on Remote Sensing of Arid and Semi-Arid Lands*, Cairo, Egypt, January, p. 973.

TUCKER, C. J., HIELKEMA, J., and ROFFEY, J., 1985 a, Satellite remote sensing of ecological conditions for desert locust survey and forecasting. *Int. J. remote Sensing*, **6**, 127.

TUCKER, C. J., TOWNSHEND, J. R. G., and GOFF, T. E., 1985 b, African land cover classifications using satellite data. *Science, N.Y.*, **227**, 369.

TUCKER, C. J., VANPRAET, C., BOERWINKEL, E., and GASTON, A., 1983, Satellite remote sensing of total dry matter production in the Senegalese Sahel. *Remote Sensing Environ.*, **13**, 461.